

Scratch Durability of Automotive Clear Coatings: A Quantitative, Reliable and Robust Methodology

Vincent Jardret, B.N. Lucas, and Warren Oliver—MTS Nano Instruments Innovation Center*
A.C. Ramamurthy—Visteon Automotive Systems†

INTRODUCTION

Automotive paint finishes are highly engineered, multi-layered polymer coatings. Customer expectations for paint finishes range from maintaining cosmetic appeal to functional performance. Deterioration of paint system performance can be linked to “chemical” stability or to “mechanical” integrity. Effects of acid rain, car wash chemicals, and UV radiation impact chemical durability, while a host of tribological scenarios encountered by painted exteriors can be linked to mechanical durability.

Tribological events of concern for painted exteriors include stone impact damage,¹ erosion by small hard particles,² micro-abrasion, also referred to in the industry as “mar,”³ adhesive wear of painted plastics,⁴ erosion durability of painted plastics subject to high pressure water jets,⁵ and scratching of paint. These concerns (chemical and mechanical) for paint durability represent diverse and complex phenomenon, which are functions of a number of variables including paint processing conditions, such as bake time and temperature.

Scratch durability of OEM automotive paint finishes is an area of significant concern to the automobile manufacturer and the paint supplier. This concern stems from direct response of customers who are known to be sensitive to these defects during the first two years of ownership. Customer concern for scratches are usually monitored by durability tracking survey (DTS) database or via clinics specially designed to understand owner complaints and perceptions which are typically supported with quantitative measurements.

An optical characterization of field scratches indicates a locus of failure within the top 50 μm . Hence, current research and development efforts are geared towards improving scratch durability of clear coatings. Scratching of clear coatings has been attributed to in-plant finessing, contact with keys, finger nails, shrubbery, routine hand washing, and commercial car washes. Published accounts include a quantitative optical method to determine scratch intensity,⁶ simulation of European car wash environments,^{7,8} real world evaluation of U.S.

Scratch and mar durability of clear coatings are issues of concern to the automobile manufacturer and paint supplier. Scratching of clearcoats is a consequence of tribological events encountered by painted exteriors during normal service life. Several subjective methods to assess scratch durability have been proposed. These methods offer little insight into scratch mechanisms. More recently, single scratch methods have been proposed to probe clearcoat scratch mechanisms. This paper outlines a reliable and robust scratch methodology for evaluating scratch durability of automotive clear coatings. It is shown that, with appropriate characterization of tip geometry, quantitative and reproducible critical load values can be obtained. A suggested test method for scratch durability is described.

and European car wash environments,⁹ and the use of single point scratch methods.¹⁰⁻¹⁵

With the exception of single point scratch methods, most of the work in scratch durability attempts to establish general trends by which automotive manufacturers rank different paint systems. These general trends seem unable to efficiently predict the performance of the paints; they bring little understanding to the actual scratch process, and also fail to identify parameters that control scratch mechanisms. In summary, knowledge in this area is preliminary and at the present time there exists no reliable and quantitative test for scratch durability of OEM automotive clear coatings.

This paper focuses on understanding the scratch behavior of OEM automotive clearcoats. Several OEM clear

*Oak Ridge TN.
†401 Southfield Rd. A108L Dearborn MI 48121-6231.

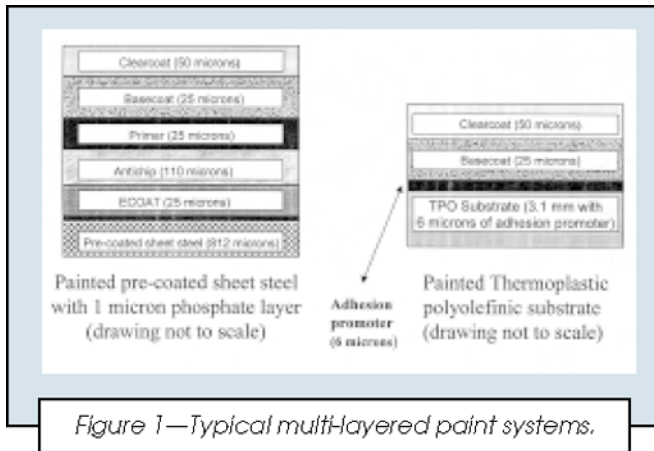


Figure 1—Typical multi-layered paint systems.

coatings have been examined for deformation under light loading and fracture behavior at higher loads. Issues associated with reliable and robust scratch measurements are discussed along with a preliminary proposal for a scratch durability metric.

PAINT SYSTEMS INVOLVED

Figure 1 shows a diagram for typical multi-layered, painted, metallic, and plastic substrates. Painted specimens consisted of all the layers, but were formulated with a black basecoat for improved visibility. Clear coatings investigated in this work were current commercial systems used at various assembly plants. Both one-component (1K) and two-component systems (2K) were included in this work. Specimens studied were tested between two and four months after their actual application. Unless specified, all the specimens were baked under normal bake time and temperature conditions.

In preparation for testing, each sample was rinsed under water to remove most dust particles, cleaned with soap to remove surface grease, and rinsed again with running water. The remaining water was then blown off with a clean air spray.

The samples designated by letters (i.e., A, B, C) distinguish the paint suppliers, while numbers denote several paints from the same supplier. In this paper, results for

fracture behavior are comprised of six paints (optimized for sheet steels) from three suppliers, including five 1K and one 2K systems. Results for ductile and viscoplastic relaxation include eight paints: five 1K and three 2K systems.

OPTICAL ASPECT OF SCRATCH VISIBILITY CHARACTERIZATION

Using car wash simulations and classical abrasion tests, previous studies relied on a measurement of the gloss retention as a criterion for paint scratch-resistance.^{7,8} The assumption is that the number of scratches present on the painted surface and their intensity are related to the amount of light diffracted outside the direct reflective angle where the gloss measurement is made. One major drawback to this kind of measurement is the large number of scratches required to significantly change the amount of diffracted light. Therefore, when using the car wash simulation technique, one increases the severity (use of abrasive slurries) and length of the test to create enough number of scratches. By doing so, simulated conditions can deviate significantly from the real world car wash conditions, thus providing misleading results.⁹

More recent studies analyze the visibility of individual scratches made under different load conditions. The idea is to estimate a load below which a scratch is no longer visible to the human eye. These studies show that a subjectivity factor must be taken into account, since this critical load value is dependent on observation time.¹⁴ In order to ascertain the influence of scratch mechanism on visibility, tests were performed wherein scratches were created under varying load conditions. As mentioned by other authors,¹⁴ some scratches were very visible within short observation times. For other scratches, one required several seconds to actually locate them. With some practice, it became easier to spot smaller scratches. This indicates that measurements of scratch visibility is a complex phenomenon with a number of undetermined parameters.

While studying scratches created under different conditions, trends were found between scratch morphology and visibility. Some of these scratches were fractured, irregular, and involved particle loss; others were smooth, regular, and involved only elastic and plastic deformation. A major consistent and noticeable difference between fractured and plastic scratches is that fractured scratches are visible independent of the incident light and observation direction. Conversely, the ductile and regular scratches are visible only under certain lighting conditions. If the scratch direction coincides with the observation and lighting directions, the scratch is not visible. When the sample is turned 90°, the scratch reappears. This is the first observation relating the scratch mechanism to visibility (Figure 2).

Scratch morphology seems to play an important role with visibility. This study focuses on mechanical aspects of characterization and is intended to provide insights into various scratch mechanisms.

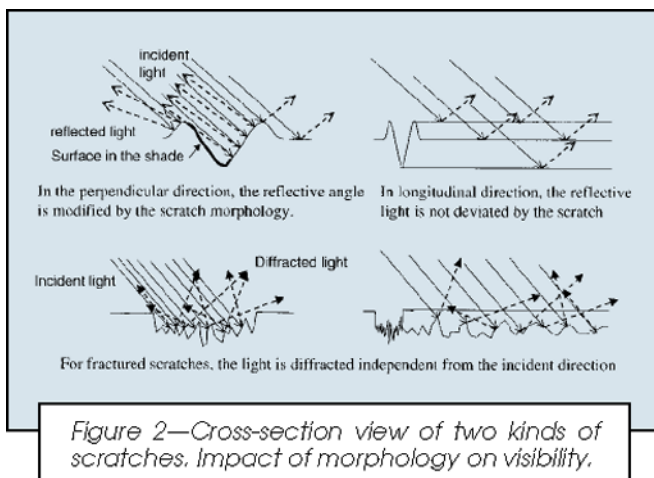


Figure 2—Cross-section view of two kinds of scratches. Impact of morphology on visibility.

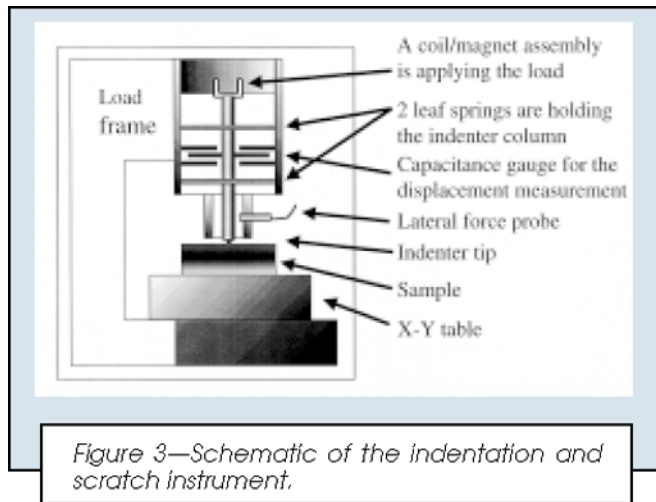


Figure 3—Schematic of the indentation and scratch instrument.

SINGLE-POINT SCRATCH TESTING: INSTRUMENTATION AND EXPERIMENTAL PROCEDURE

Originally developed for depth-sensing indentation testing purposes,¹⁶⁻¹⁸ the Nano Indenter XP[®] was used to perform the scratch experiments described and analyzed in this work. The indentation head of this instrument is load controlled. The load is applied normal to the sample surface by a magnet/coil system, allowing for precise and fast control (Figure 3). The indenter column is held by two leaf springs, which offer very low stiffness to the indenter's perpendicular motion. The maximum distance allowed for the indenter travel, normal to the sample surface, is about 1.5 mm. Over this entire range, displacement resolution is less than 0.1 nm. Maximum load capacity for the standard system is 500 mN with a precision of less than a micro-Newton. This loading precision includes the accuracy of a contact-detection algorithm, which determines the point of first contact between the surface and the indenter and also determines the corresponding zero-load reference. A high-load option can be added to the standard indentation head configuration, allowing the system to achieve loads up to 10 N.

The lateral force measurement (LFM) option available on this instrument measures the forces in the perpendicular direction to the indenter column. During a scratch test, these forces correspond to tangential frictional force and to the lateral scratch force (see Figure 4). This in turn allows an estimation of the friction coefficient for scratches made in any direction. The precision for frictional force measurement is better than 10 μ N over a range of 200 mN. High-precision screw driven tables were used to ensure smoothness in scratch and profile motion.

During a scratch test, the normal force on the indenter is controlled and can be held constant or increased/decreased at a linear rate. The design of the instrument used makes the force generated at the tip a very small function of the vertical displacement of the indenter. Only small corrections are needed and made to the load due to this vertical motion. The small mass of the indenter holder reduces the effects of dynamic motion on the load applied on the sample. This feature allows the

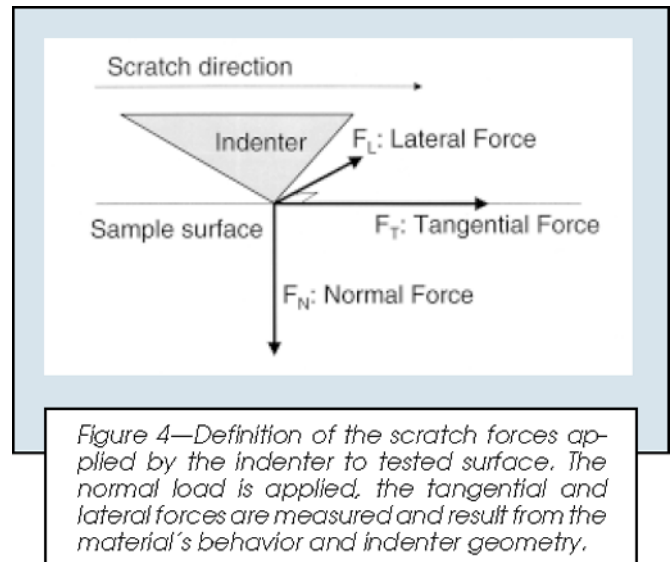


Figure 4—Definition of the scratch forces applied by the indenter to tested surface. The normal load is applied, the tangential and lateral forces are measured and result from the material's behavior and indenter geometry.

application of a precisely controlled load during a lengthy scratch experiment even for rough or curved surfaces. Scratch velocity and scratch path followed by the indenter on the specimen surface are defined by the operator. Scratch velocity is typically held constant throughout the scratch experiment and can be set between 0.05 μ m/s to 2.5 mm/s. For these tests, a velocity of 25 μ m/s was used. Any arbitrary path can be defined by joining a series of points via straight line segments.

The design of the indenter tip mount allows the operator to replace tips easily and remount them in the same position each time. This is a very useful feature for studying clearcoat scratching where the indenter geometry has a great influence on the scratch behavior, as shown in the following.

A typical scratch experiment is performed in three stages: a pre-profile, a scratch segment, and a post-profile. Indenter's actual penetration depth under the sample surface is estimated by comparing the indenter's dis-

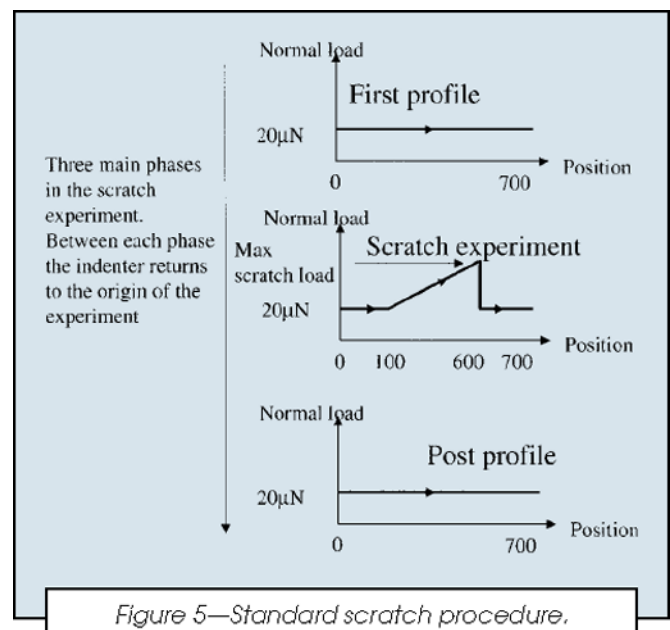


Figure 5—Standard scratch procedure.

placement normal to the surface during the scratching, with the altitude of the original surface at each position along the scratch length. The original surface morphology is obtained by pre-profiling the surface under a very small load at a location where the scratch is intended to be placed. Roughness and slope of the surface are taken into account in the calculation of the indenter penetration. In a similar manner, a post-profile helps establish residual scratch depth (see *Figure 5*).

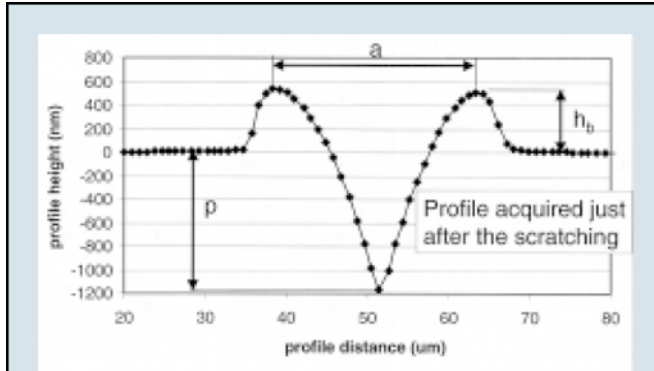


Figure 6—Cross profile over a scratch; definitions: a —scratch width, h_b —pile-up height, p —scratch depth.

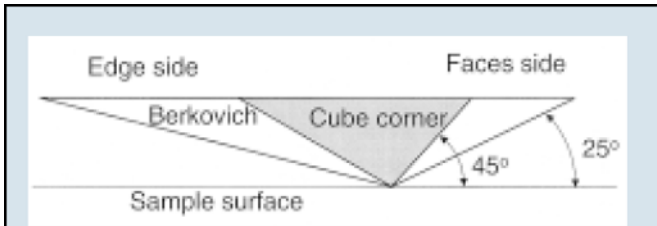


Figure 7—Definition of the attack angle. Angle between the indenter face and the sample surface. Comparison of the Berkovich with the cube corner indenter.

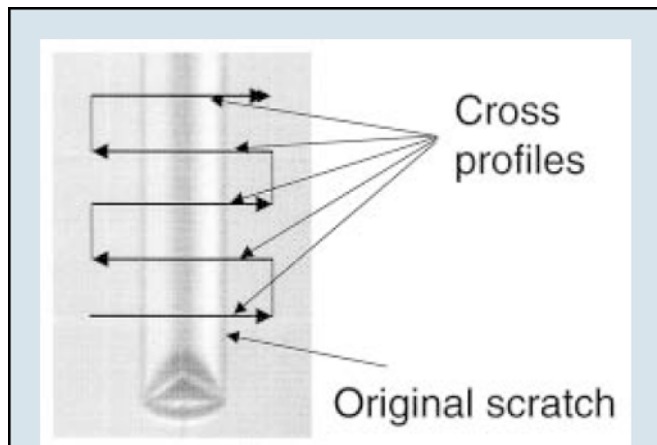


Figure 8—Cross profiles are performed after a scratch experiment. Five profiles are usually used for each scratch.

Additional morphological information can be determined by profiling across the scratch (see *Figure 6*). Knowledge of load and penetration depth are vital in any scratch testing, but when ductile mechanisms are involved in the abrasion process, a measurement of residual scratch depth, width, and pile-up height allows us to estimate scratch contact-pressure and the actual friction coefficient.¹⁵ Both scratch and profile procedures can be integrated into a single-scratch experiment, allowing for automated data reduction.

Review of Scratch Mechanisms

Identification of scratch mechanisms is accomplished using an optical microscope mounted in the instrument. Using the system's positioning tables, observed morphology can be related to the evolution of penetration and tangential force curves. Three main scratch mechanisms were identified using different indenter geometries. Elastic-plastic deformation can be observed under mild abrasive conditions (e.g., where the attack angles are small or when experiments are carried out with a Berkovich indenter) (see *Figure 7*). Irregular fracture processes occur when the attack angle is larger (e.g., with a cube corner indenter with its face in the direction of the scratch). When a cube corner indenter is used with its edge in the direction of the scratch, a regular longitudinal fracture propagates in front of the indenter. The indenter seems to open this crack in front like a knife.

In order to quantify these three behaviors, experiments were conducted where the normal load, normal indenter displacement, tangential force, and indenter position on the sample are measured during the experiments. These measurements aid in delineating scratch mechanisms.

Plastically Deformed Scratches

Under mild abrasive (loading) conditions, scratches on clearcoats undergo elastic-plastic deformation, which leads to a groove accompanied by two lateral pile-up pads. These scratches are very regular along the scratch length. This scratch behavior has been extensively studied by Jardret et al.¹⁶

Plastically deformed scratches can be described using the following relevant parameters: pile-up height over scratch width; residual depth over total penetration depth; scratch width; and scratch contact pressure.

These parameters can be measured immediately after the scratch is made by performing a cross-profile measurement. Several profiles performed on the same scratch increases the statistical significance of the results (*Figure 8*).

Indenter geometry has a strong effect on elastic-plastic deformation morphology. *Figure 9* illustrates the effect of the orientation of a Berkovich indenter on the residual scratch morphology. The pile-up formation is much less evident when the edge of the Berkovich indenter is oriented in the scratch direction. It is interesting to note here that indenter's penetration depth does not strongly depend on its orientation. This result is confirmed by comparing scratch morphologies using

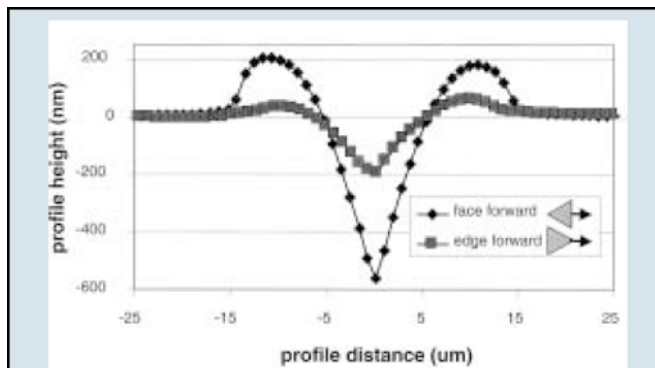


Figure 9—Influence of the contact geometry on the residual scratch shape for scratches performed under the same normal load and at the same velocity.

Berkovich and cube corner indenters. Cube corner indenters create a much larger pile-up than Berkovich for equivalent scratch width or normal applied loads.

Time-dependent properties of polymer materials have been studied extensively, yet only a few studies are reported for time dependence in mechanical characterization of surfaces.²⁰⁻²¹ During a scratch test, two time-dependent processes, visco-plastic deformation and visco-elastic relaxation, occur. These processes have a strong influence on scratch morphology and can be characterized quantitatively. Visco-plastic processes are related to a polymer's sensitivity to deformation rate being applied to the surface. For a given indenter geometry and penetration depth, this rate is related to scratch velocity. Maintaining the same normal load, variation in scratch velocity results in a corresponding variation in the resulting scratch width. Faster motion results in a thinner residual scratch.²² Relaxation processes (healing) are important when a scratch is left at room temperature for some period of time. This phenomenon affects only dimensions normal to the surface and the scratch width remains unchanged, as shown in *Figure 10*. These samples were stored at room temperature in a cabinet for 15 days after the scratches were made. The observed relaxation was significant and showed a reduction of up to 50% in pile-up height for some of the samples (see *Figure 11*).

Time-dependent properties are also usually associated with temperature-dependent properties, hence, the effect of an elevated temperature on the residual shape of a scratch was investigated. We submitted the same samples (used in *Figure 10*) to eight hours at 40°C, to observe the effect of elevated temperatures on the degree of relaxation. This experiment showed that most of the scratches relaxed, resulting in a further reduction in pile-up height. Scratch width, however, remained constant (*Figures 10 and 11*).

Scratch visibility in the real world is significantly influenced by clearcoat relaxation phenomenon. A ductile scratch on a car may be visible initially but after the day under the hot sun, this scratch may no longer be visible, due to the relaxation of the clearcoat surface. It is worth noting that the temperature of a car body during a hot summer day can easily reach 50° to 60°C. In our quest

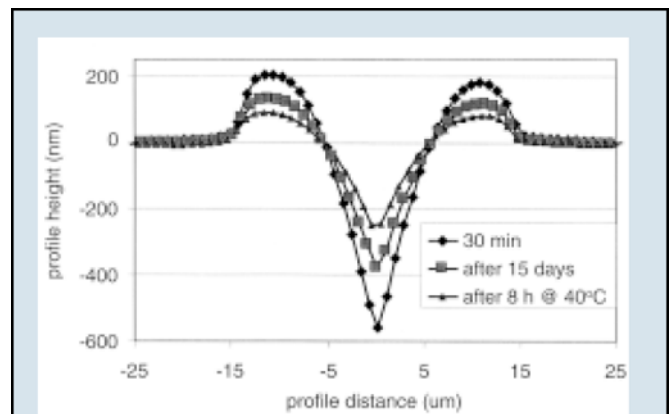


Figure 10—Visco-plastic recovery of a ductile scratch with time and temperature.

for identifying parameters that would correlate to scratch visibility, it is important to state that, even though the scratch width remained unchanged, visibility decreased with a decrease in pile-up height and residual scratch depth.

Fractured Scratches

Clearcoat fracture is observed using cube corner indenters. Using the edge of a cube corner indenter in the scratch direction, clearcoat surfaces are cut in the centerline of the groove, as shown in *Figure 12*. Along this longitudinal crack, propagating in front of the indenter motion, elastic-plastic deformation takes place in a fashion similar to that described in the previous section. Plastic deformation around the middle crack is subject to relaxation, and the residual pattern of the scratch after relaxation is a thin regular line, corresponding to median fracture. With an indenter whose radius of curvature is between 0.5 to 2 μm, this middle crack initiates only under high loads, from 2 to 10 mN. This transition from not-cracked to cracked behavior does not appear clearly on the scratch curves (penetration and tangential force curves).

Using a sharp cube corner indenter with its face oriented in the scratch direction, an irregular fracture pro-

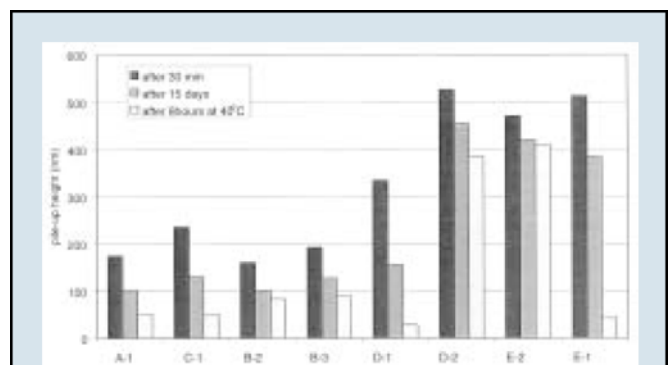


Figure 11—Effect of visco-plastic relaxation on the residual scratch pile-up height.

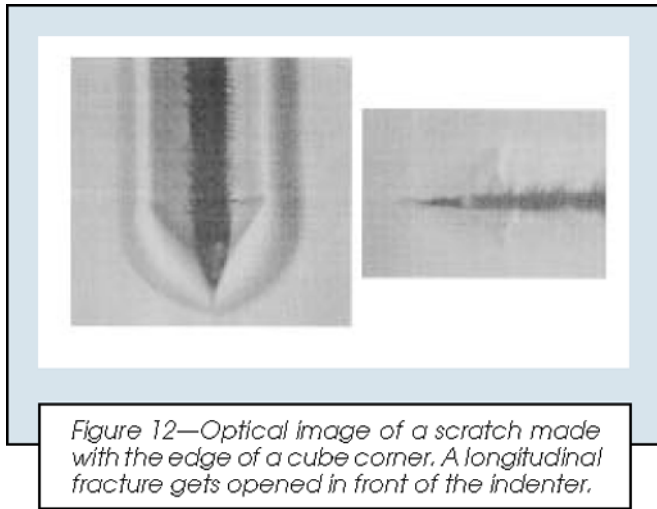


Figure 12—Optical image of a scratch made with the edge of a cube corner. A longitudinal fracture gets opened in front of the indenter.

cess occurs. Particles are chipped out of the surface. This behavior creates irregularities in scratch penetration, tangential force curves, and residual scratch morphology. This irregular fracture behavior generates material loss from the surface, hence, relaxation does not restore the original surface morphology. Visibility of these scratches does not change with time, even at elevated temperatures.

The Berkovich indenter, with an angle of 25° , only results in plastic and elastic deformation, while the cube corner, with an angle of 45° , induces fracture damage. Clearly, at some angle, cracks start to be generated in the scratch. To observe this phenomenon, the sample was tilted and a cube corner indenter was used to create a scratch under a constant load of 40 mN. Starting from an attack angle of 25° , the angle was increased with steps of 5° by tilting the sample surface. Most clearcoats started to crack between 30° and 40° . First, chevron-shape fractures propagate from the center of the groove toward the edge of the scratch (Figure 13). Then, chips and par-



Figure 13—Optical image of a scratch made by the face of a cube corner. The sample surface is tilted 10° .

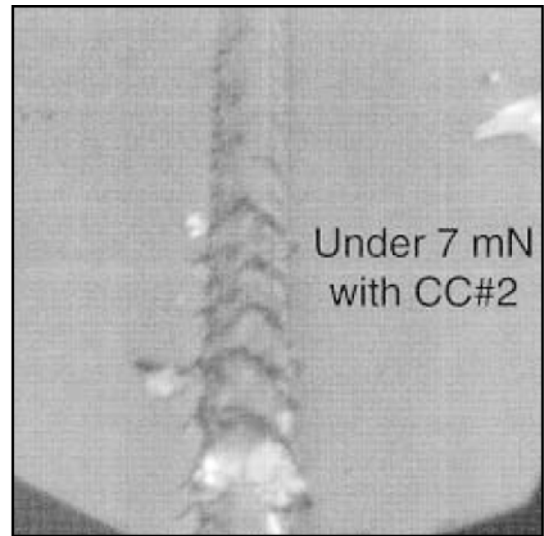


Figure 14—Fracture behavior on sample 2B (TK).

ticles start to be formed and detach from the surface. These experiments confirmed the results presented previously by Briscoe.²⁰

Transition between smooth ductile to irregularly fractured scratch behavior can also take place when an increasing load is applied to a cube corner indenter. Under small loads, scratches are smooth and ductile and above a certain critical load, L_c , scratches are fractured (see Figures 14 and 15). The indenter penetration depth under the critical load, D_c , can also be an important parameter to characterize the contact geometry. All real indenters have some tip rounding, therefore, as the penetration of the indenter increases, the actual angle of attack increases as well. This result tends to indicate that critical load is related to the change of the equivalent attack-angle induced by the indenter's penetration under the surface. The effect of indenter's sharpness on the critical load value for a given material is additional evidence for the relationship between the critical load and attack angle. However, this feature is not fully understood at this point, and other parameters may have a significant influence on this relation.

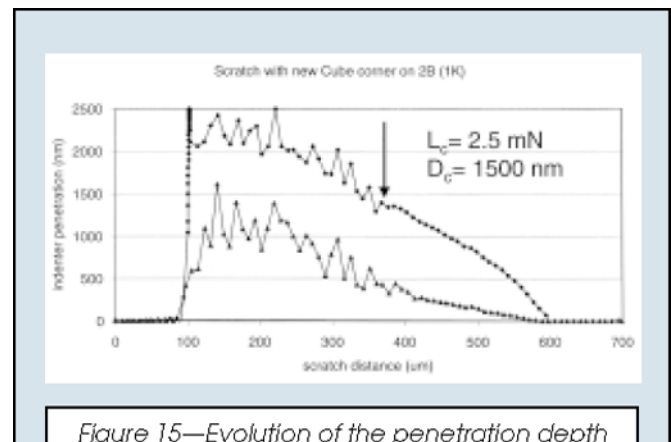


Figure 15—Evolution of the penetration depth during a ramp load scratch showing the ductile to fracture transition in the paint behavior.

If higher critical-load values correspond to better paint performance, then relation between single-scratch behavior and real world scratch resistance of clearcoats can be correlated.

RESULTS AND DISCUSSION

A careful study of real world scratch morphologies reveals that most scratches created by car washing are fractured scratches.⁶ These data indicate that ductile behavior of clearcoats should not be responsible for a large part of the scratch problem, as our results on the relaxation of ductile scratches also pointed out, given the high temperatures the body of a car easily reaches under the radiation of the sun.

Figure 16 shows critical load (for fracture) data obtained using a cube corner indenter for several OEM clear coatings. Ranking obtained by this method is in excellent correlation with field data obtained for several vehicle lines over a period of five years. Figure 16 closely tracks the durability tracking survey (DTS) data with least customer complaints received for clear coatings with high critical loads. Higher critical load values relate with fewer customer complaints. This observation supports the proposition that customer satisfaction is strongly related to a clearcoat's ability to resist initiation and propagation of fracture phenomena under abrasive conditions.

Among the parameters related to plastic deformation (e.g., pile-up height, scratch width, residual scratch depth, ability to relax with time and temperature), we have found no strong correlation with customer satisfaction data. One reason for this may be that relaxation phenomenon described earlier reduces the probability of noticing a ductile scratch. However, at lower temperatures, plastically deformed scratches may not relax as much or as quickly and hence may be important in certain real world conditions.

Robustness and Reproducibility: Critical Role Played by Indenter Geometry in Critical Load Measurements

The effect of the curvature at the indenter tip on critical load measurements for paint is presented in Figure 17. Reliable and reproducible scratch measurements require the availability of indenters with reproducible tip geometry, such that results from a scratch test are not akin to this specific indenter. Position and control of the indenter geometry is a major challenge for any scratch technique, and this section addresses this issue and proposes a few solutions which may be used in an industrial environment.

Critical load measurements require indenters with a certain curvature of their extremity, as shown previously. Conical indenters have been widely used to date. Their advantage is the axi-symmetric characteristic of their geometry. For those made of diamond, several major problems still exist. First, the crystallographic structure of a diamond is not compatible with a conical shape, and it is very difficult to reproduce exactly the same

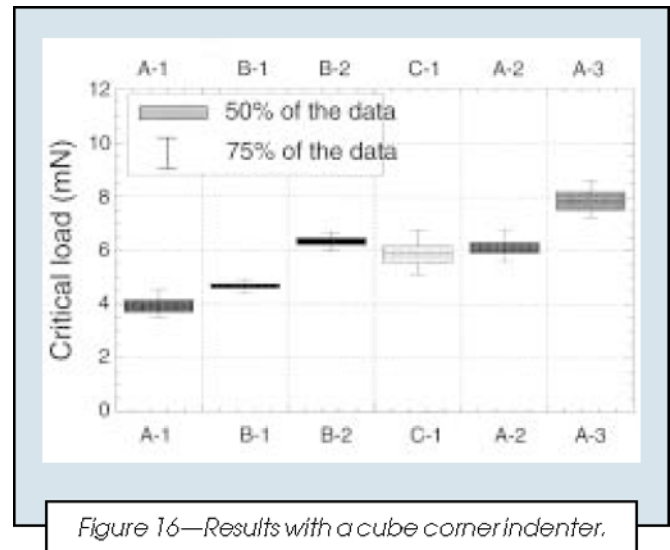


Figure 16—Results with a cube corner indenter.

conical shape in each indenter. Also, the texture of a conical-shaped indenter remains rough, independent of the polishing process. This rough texture will strongly affect the indenter's intimate friction behavior when used in a scratch test. The rounding of diamond conical indenters is usually not reproducible. Also, conical indenters can dramatically change in geometry after wear or polishing process and transform to a four-faced pyramid at the tip.

Pyramidal indenters, like Berkovich, have been widely used in indentation studies. Their reproducibility allowed a standardization of their shape; therefore, critical load values did not show a dramatic change from one indenter to another. The advantage of pyramidal indenters is that their geometry and texture can be controlled easily, angles for the faces measured accurately, and the faces themselves optically polished. Three-faced pyramids, like Berkovich and cube corner indenters, allow a very sharp geometry with a radius of curvature of less than 50 nm. The development of nano-indentation technology has allowed accurate measurement of such features. This measurement follows the analysis presented by Oliver and Pharr.^{1b} Relation between the contact stiff-

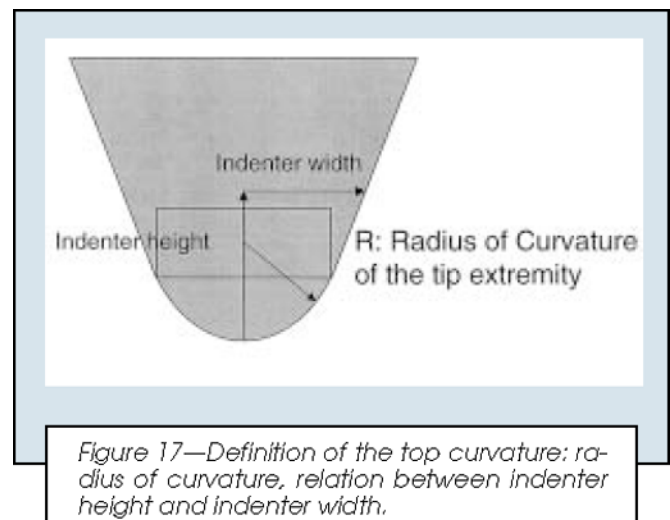


Figure 17—Definition of the top curvature: radius of curvature, relation between indenter height and indenter width.

ness and the contact depth during a nano-indentation experiment describes the geometry of the indenter. This relation is obtained from an indentation test using fused silica whose modulus is 72 GPa. The contact stiffness (S) is related to the contact area (A) and the material's elastic modulus (E) by

$$S = \frac{2\sqrt{A}}{\sqrt{\pi E}} \quad (1)$$

The contact area is usually calculated from the contact depth (h_c) with

$$A = 24.56h_c^2 + \sum_{i=0}^9 C_i h_c^{i/2} \quad (2)$$

with
$$h_c = h - 0.75 \frac{P}{S} \quad (3)$$

where P is the normal load and h the indenter penetration depth. The coefficient 24.56 describes the angle of the indenter faces. The following terms, $C_i h_c^{i/2}$, are used to take the rounding of the tip into account at small depths. Also, the contact area can be described using a circular model by an equivalent contact radius (a).

$$a = \frac{SE}{2} \quad (4)$$

As the elastic modulus of silica is constant as a function of depth, the contact radius is directly proportional to the contact stiffness. A plot of equivalent contact radius versus contact depth derived from an indentation experiment on fused silica illustrating the geometry of the indenter is shown in *Figure 18* for four different cube corner indenters.

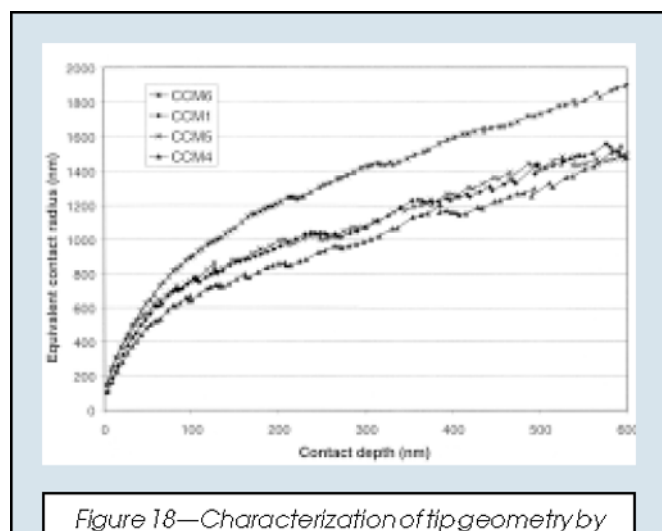


*Figure 18—Characterization of tip geometry by indentation. The graph shows two identical indenters CCM1 and CCM5. CCM4 is sharper and CCM6 is blunter. Their geometries correspond to different values of critical load as shown on *Figure 19*.*

Cube corner indenters with specific radii of curvature manufactured with a good degree of reproducibility were used in this work. Using cube corner indenters, it is possible to extend the range of radius of curvature from 50 nm to several micrometers. Reproducibility and control of this manufacturing process can be assessed using indentation testing on standard materials, as described previously (*Figures 18* and *19*). Critical load measurements on automotive clear coatings show that the differences between several indenter tips remain within the scatter range reported earlier (*Figure 20*) using one indenter tip.

Scatter Associated with Critical Load Measurements

Experimental scatter in critical load values was estimated using classical statistical procedures. In our scratch experiments, a cumulative average for critical loads reaches a steady value after about 20 scratches. The deviation in critical-load values is dependent upon paint type. Scatter has been found to be as low as three percent for some paints, but reach 10% in others. As illustrated in *Figure 16*, critical load variations between current commercial automotive clearcoats are not very large. Hence, it is necessary to perform a minimum number of experiments to objectively distinguish clearcoats from one other. Several cube corner indenters with different sharpnesses were used on all tested samples. These experiments show that the indenter geometry does not change the ranking of clearcoats when the same indenter geometry is used; however, the critical load values do change when the indenter geometry is changed (*Figure 19*). The difference between critical-load measurements with several tips of identical radii of curvature is smaller than seven percent, while for a given tip, the deviation in the critical load is between three percent and 10%. For some paints, the difference between tips is smaller than three percent. Since small differences in the indenter's geometry can affect critical load by 20% or more, it is mandatory to characterize indenter geometry in any reporting of scratch durability.

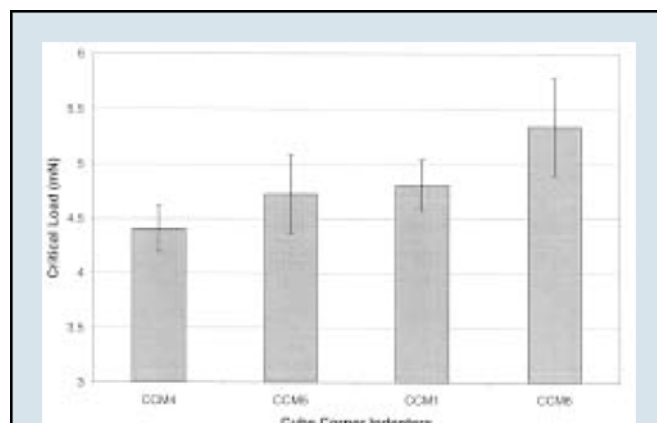


*Figure 19—Critical load values obtained for one paint with various cube corner indenters which geometries are shown on *Figure 18*.*

Proposed Test Method for Determination of Automotive Clear Coatings' Scratch Durability

Our discussion clearly establishes the need for a reliable, robust, and quantitative test method for evaluating OEM clearcoat scratch durability. The proposed scratch method involves measuring critical load for fracture using cube corner indenters with a well-characterized tip geometry and with the face oriented in the scratch direction. Twenty individual scratches provide a statistically significant steady state value for the critical load. The displacement normal to the clearcoat's surface is measured during the test.

Each scratch test consists of

- A profile of 500 μm , under a normal load of 20 μN at a velocity of 25 $\mu\text{m/s}$,
- A ramping-load scratch segment in which the load is increased from 20 μN at a rate of 800 $\mu\text{N/s}$, up to a normal load of 16 mN, at a velocity of 25 $\mu\text{m/s}$.

A critical load value for each scratch test is calculated based on the indenter's penetration curve. The critical load value corresponds to an increase in noise during penetration of the clear coating. Average and standard deviations for critical load value are estimated over these 20 scratches.

We have been able to characterize a clearcoat specimen within 30 min, including sample loading, testing, and data-reduction. Several samples can be studied in one run; automated operation allows as many as 10 samples to be studied overnight.

For reasons outlined in the previous section, indenter geometry must regularly be checked using an indentation experiment on fused silica. Normal load (P) and the elastic contact stiffness (S) should be measured along with the displacement normal to the silica surface (h). Relation between contact stiffness (S) and contact depth (h_c) should be evaluated using equation (3) and correlated to the critical load results.

CONCLUSIONS

A quantitative, reliable, and robust method for measuring critical load for clearcoat fracture has been described. Critical loads measured show very good correlation with durability tracking survey (DTS) data.

Critical load measurements are strongly influenced by tip geometry. Hence, it is mandatory to characterize tip geometry in order to ensure the robustness of this measurement. For well-characterized indenters, it is necessary to determine an optimum number of scratch experiments to obtain statistically significant critical load values. The knowledge of the indenter shape associated with the critical load measurement results render critical load values quantitative and allow others to reproduce the measurement in the exact same conditions. Reliability of this test is ensured by the availability of both identical indenters and an accurate, well-established method to control their geometry.

Although critical load measurements have been shown to be reproducible and robust, it is still difficult to relate

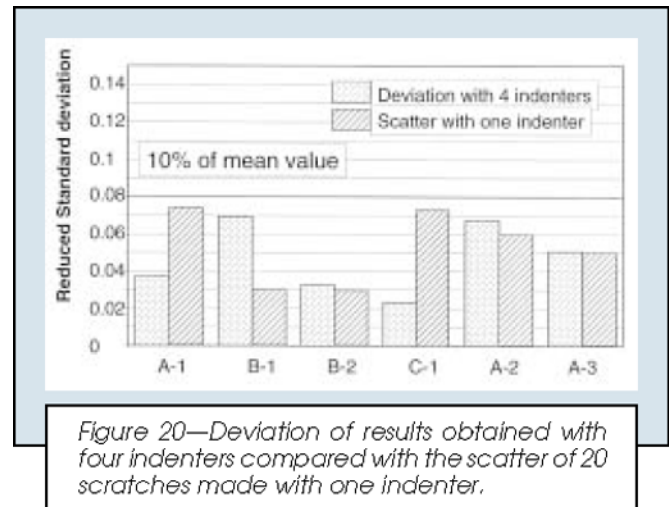


Figure 20—Deviation of results obtained with four indenters compared with the scatter of 20 scratches made with one indenter.

the critical load values to intrinsic mechanical properties of the polymer surface. Also, for applications where thinner films are involved, the interaction between the radius of curvature of the indenter tip and the thickness of the film will add to the complexity of this test.

ACKNOWLEDGMENTS

The authors would like to acknowledge guidance, support, and interest by Ford Motor Company.

References

- (1) Pamamurthy, A.C., Buresh, G.A., Nagy, M., and Howell, M., "Novel Instrumentation for Evaluating Stone Impact Wear of Automotive Faint Systems," *Wear*, 225, 936 (1999).
- (2) Putherford, K.L., Trezona, P.I., Hutchings, I.M., and Pamamurthy, A.C., "The Abrasive and Erosive Wear of Polymeric Faint Films," *Wear*, 203, 325 (1997).
- (3) Pickles, M.J., Trezona, P.I., Hutchings, I.M., Pamamurthy, A.C., and Freese, J.W., "New Methods for Characterizing the Mechanical Durability of Automobile Faint Films," SAE International, Paper 980977, Detroit, MI, 1998.
- (4) Pamamurthy, A.C., Charest, J.A., Lilly, M.D., Mihora, D.J., and Freese, J.W., "Friction Induced Faint Damage—A Novel Method for Objective Assessment of Painted Engineering Plastics," *Wear*, 203, 350 (1997).
- (5) Pamamurthy, A.C., Buresh, G., Jones, A., Shah, S., Szczepaniak, E., Edge, D., Freese, J.W., and Linberg, F., "Durability of Painted Automotive Exteriors Subject to High-Pressure Water Jets—Simulation of Free Car Wash Environments," SAE International, Paper 980974, Detroit, MI, 1998.
- (6) Ottiviani, P.A., Iyengar, V., and Cheever, G.D., "Use of the Goniphotometer for Scratch and Mar Testing of Automotive Topcoats," SAE International, Paper 970988, Detroit, MI, 1997.
- (7) Potter, F.A., Jacobs, F.B., Engbert, T., and Bock, M., "Scratching of Automotive OEM Clearcoats—Method and Media Effects," SAE International, Paper 980975, Detroit, MI, 1998.
- (8) Jacobs, F.B. and Engbert, T., "Studies on Scratch and Mar Resistance of Polyurethane Coatings," SAE International, Paper 960913, Detroit, MI, 1996.
- (9) Pamamurthy, A.C., Buresh, G.A., Buresh, J., Moorehead, F., Gale, L., and Belanger, L., *Proc. ACT 99 Conference*, The Engineering Society of Detroit, Detroit, MI, September 1999.
- (10) Shen, W., Smith, S.M., Jones, F.N., and Ji, C., "Use of a Scanning Probe Microscope to Measure Marring Mechanisms and Microhardness of Crosslinked Coatings," *JOURNAL OF COATINGS TECHNOLOGY*, 60, No. 373, 123 (1997).

- (11) Ryntz, R., Abell, B.D., and Hermosillo, F., "Scratch Resistance of Automotive Plastic Coatings," SAE International, Detroit, MI, 1998.
- (12) Jones, F.N., Shen, W., Smith, S.M., Huang, Z., and Ryntz, R.A., *Prog. Org. Coat.*, 34, 119 (1998).
- (13) Adamson, K.G., Blackman, G., Gregorovich, B., Lin, L., and Matheson, R., "Oligomers in the Evolution of Automotive Clearcoats," *Prog. Org. Coat.*, 34, 64-74 (1998).
- (14) Blackman, G.S., Lin, L., and Matheson, R.R., "Micro-Mechanical Characterization of Mar Behavior of Automotive Topcoats: Micro and Nano-Wear of Polymeric Materials," *Proc. Polym. Prep. (Am. Chem. Soc., Div. Polym. Chem.)*, 39, No. 2, 1224 (1998).
- (15) Blackman, G.S., Lin, L., and Matheson, R.A., "Micro and Nano Wear of Polymeric Materials," *Proc. Polym. Prep. (Am. Chem. Soc., Div. Polym. Chem.)*, p. 1218, Boston, 1998.
- (16) Oliver, W. and Pharr, G.M., "An Improvement for Determining Hardness and Elastic Modulus Using Load and Displacement Sensing Indentation Experiments," *J. Mater. Res.*, Vol. 7, No. 6, June 1992.
- (17) Lucas, B., Oliver, W., Pharr, G.M., and Loubet, J.L., "Time Dependent Deformation During Indentation Testing," *Proc. Mat. Res. Soc. Symp.*, 436, 1997.
- (18) Lucas, B., Oliver, W.C., and Ramamurthy, A.C., "Spatially Resolved Mechanical Properties of a "TPC" Using a Frequency Specific Depth-Sensing Indentation Technique," *Proc. Antec 97*, Volume III, Society of Plastic Engineers, 1997.
- (19) Jardret, V., Zahouani, H., Loubet, J.L., and Mathia, T.G., "Understanding and Quantification of Elastic and Plastic Deformation during a Scratch Test," *Wear*, 218, 8-14 (1998).
- (20) Briscoe, B., Evans, P.D., Pelillo, E., and Sinha, S.K., "Scratching Maps for Polymers," *Wear*, Vol 200, 1996.
- (21) Lucas, B., Oliver, W.C., Pharr, G.M., and Loubet, J.L., "Time Dependent Deformation During Indentation Testing," *Proc. Mat. Res. Soc. Symp.*, Vol 436, 1997.
- (22) Jardret, V. and Oliver, W.C., "Thin Films: Stresses and Mechanical Properties," *Proc. Mater. Res. Soc. Symp.*, 594, Boston, MA, 1999.